Environmental Microbiome

RESEARCH

Open Access

Salinization alters microbial methane cycling in freshwater sediments

Lorena Selak[1,2], Dimitri V. Meier[3], Maja Marinović[1,4], Andrea Čačković[1], Katarina Kajan[1,5], Petra Pjevac[6,7*†] and Sandi Orlić[1,5*†]

Abstract

Climate change–induced salinization poses a global threat to freshwater ecosystems and challenges microbial communities driving crucial biogeochemical processes, particularly methane cycling. This study examined the impact of salinization and the accompanying sulfate concentration increases on microbial community dynamics and methane cycling in coastal freshwater lake sediments. We show that sulfate enrichment in sediment profiles enables the proliferation of distinct sulfate-reducing bacteria (SRB) that reshape microbial niches by competing with methanogens and promoting sulfate-dependent anaerobic oxidation of methane (AOM). Freshwater SRB clusters, which compete with some methanogens for substrates but also degrade organic compounds into methanogenesis precursors, are replaced by the SEEP-SRB groups that form syntrophic relationships with ANME-1 in salinized sediments. As seawater intrudes and reshapes microbial communities, a methane pocket forms that escapes both aerobic and anaerobic oxidation. Underneath this methane pocket, SRB play a key role in enabling sulfate-dependent AOM, facilitating methane consumption at higher sediment depths. While all microorganisms demonstrated some physiological adaptability potential to elevated osmotic stress, SRB exhibited the highest resilience to increased salinity. These findings highlight how salinization-induced geochemical shifts, particularly sulfate enrichment, directly affect microbial community assembly and impact methane cycling in coastal freshwater ecosystems.

Keywords Salinization, Microbial methane cycle, Sulfate reducing bacteria, Microbial adaptations, Community shifts

†Petra Pjevac and Sandi Orlić contributed equally to this work.

*Correspondence:
Petra Pjevac
petra.pjevac@univie.ac.at
Sandi Orlić
sorlic@irb.hr
[1]Ruđer Bošković Institute, Bijenička cesta 54, Zagreb 10000, Croatia
[2]Nordic Center for Earth Evolution (NORDCEE), University of Southern Denmark, Odense, Denmark
[3]Bayreuth Center of Ecology and Environmental Research (BayCEER), Department of Ecological Microbiology, University of Bayreuth, 95448 Bayreuth, Germany
[4]BICRO BIOCentre Ltd., Borongajska cesta 83H, Zagreb 10000, Croatia
[5]Center of Excellence for Science and Technology-Integration of Mediterranean Region (STIM), Zagreb, Croatia
[6]Joint Microbiome Facility of the Medical University of Vienna, University of Vienna, Djerassiplatz 1, Vienna 1030, Austria
[7]Department of Microbiology and Ecosystem Science, Division of Microbial Ecology, University of Vienna, Djerassiplatz 1, Vienna 1030, Austria

Background

Lakes are significant natural sources of methane, one of the major greenhouse gasses [1], and together with other freshwater systems contribute up to 41% of annual global methane emissions [2]. Methane fluxes in these ecosystems depend on rates of microbial methane production and consumption, determined by the metabolic activities of methanogens, aerobic methanotrophs, and anaerobic methanotrophs (ANME). Anoxic conditions and the availability of carbon dioxide, methylated compounds, hydrogen, and acetate are important for the development of methane-producing archaeal communities [3, 4]. In lakes, methane produced in anoxic sediments diffuses upwards, where it can be oxidized by ANME in anoxic layers, or by aerobic methanotrophs in the oxic-anoxic transition zone and above [5–8].

ANME oxidize methane in syntrophy with bacterial partners using electron acceptors such as sulfate, nitrate, nitrite, and metal oxides [9, 10]. These syntrophic interactions can involve direct interspecies electron transfer (DIET) facilitated by pili and multiheme c-type cytochromes (MHC) [11]. In ocean sediments, anaerobic oxidation of methane (AOM) is primarily carried out by consortia of ANME and sulfate-reducing bacteria (SRB). Marine ANME-1 and ANME-2 archaea are commonly associated with SEEP-SRB1 or SEEP-SRB2 syntrophic partners [12–14]. AOM in freshwater systems, like wetlands and lake sediments, differs from that in marine systems. Due to the generally low sulfate levels in freshwater systems, ANME are usually less abundant and rely on nitrite-, nitrate-, and metal oxide-reducing partners [15, 16]. The very shallow sulfate-methane transition zone (SMTZ) favors methanogenesis close to the sediment surface [17]. In addition to the geochemical setting in sediments and syntrophy-driven AOM, other competitive or mutualistic interactions during anaerobic organic matter (OM) degradation affect the microbial methane cycle [18]. For example, SRB can compete with other anaerobes, including methanogens, for a wide range of substrates such as alcohols, organic acids, and hydrogen [19]. In freshwater ecosystems, despite low sulfate concentrations, cryptic sulfur cycling can, however, sustain high sulfate reduction rates, comparable to those in marine sediments. These hidden processes can contribute significantly to carbon mineralization and mitigate methane emissions [20]. The competition dynamics between SRB and methanogens depend on the availability of sulfate and the seasonal variations in the quality and quantity of OM introduced by sedimentation [21, 22].

The salinization of freshwater resources due to climate change can occur through several mechanisms. In coastal regions, rising sea levels drive saltwater intrusion into freshwater aquifers, while changes in precipitation patterns and rising temperatures generally increase evaporation and salt concentration [23]. Disturbances in the freshwater-sea interface [24] result in increased ion concentrations in both water column and sediments. Many coastal areas are threatened by salinization, which can affect the principal functions of providing freshwater, supporting biodiversity, regulating climate, and sequestering carbon [25, 26]; but also, the activity of microbial communities involved in the methane cycle by increasing the availability of alternative electron acceptors [16, 27]. Salinization can affect the establishment of syntrophic relationships between ANME and their partners and requires specific microbial adaptations to increased osmotic pressure and altered environmental conditions [28]. Increased salinity has previously been shown to reduce the diversity and interconnectivity among aerobic methanotrophs [29], but also to reduce AOM activity [30]. Recently, the introduction of brackish water conditions was found to reduce methane concentrations, despite no detectable changes in methanotroph abundance or methanogen population structure. However, a significant increase in SRB abundance was observed [31]. Moreover, nitrate-dependent AOM organisms, e.g. *Methanoperedens nitroreducens* have demonstrated tolerance to elevated salinity, by changing syntrophic partners under different salinity conditions [32]. As salinization of freshwater systems is a consequence of climate change, understanding its impact on methane dynamics in coastal environments is key to predicting future microbial responses and greenhouse gas emissions.

Coastal Lake Vrana, separated from the Adriatic Sea by a semipermeable limestone ridge (Supplementary Fig. 1a), is located in an agriculturally developed region and serves as a carbon sink, water resource, and bird sanctuary. The lake has two main canalized tributaries, one completely isolated from incoming seawater [33]. During summer, reduced inflow, high temperatures, and limited precipitation lower the water level, causing seawater intrusion. This disruption in the precipitation-evaporation balance leads to ecosystem perturbations, impacting microbial communities and carbon cycling [33, 34]. Lake Vrana thus provides an ideal natural laboratory for studying lake salinization. We hypothesized that lake salinization, through affecting sediment geochemistry, would also directly influence the diversity and distribution of sulfate-reducing and methane-cycling microorganisms. By comparing sediments unaffected and affected by seawater intrusion to improve our understanding of methane dynamics in the face of climate change. We identified striking changes in sediment geochemistry accompanied by shifts in methane-cycling microbial communities, suggesting that salinization can alter both methane production and oxidation in freshwater environments.

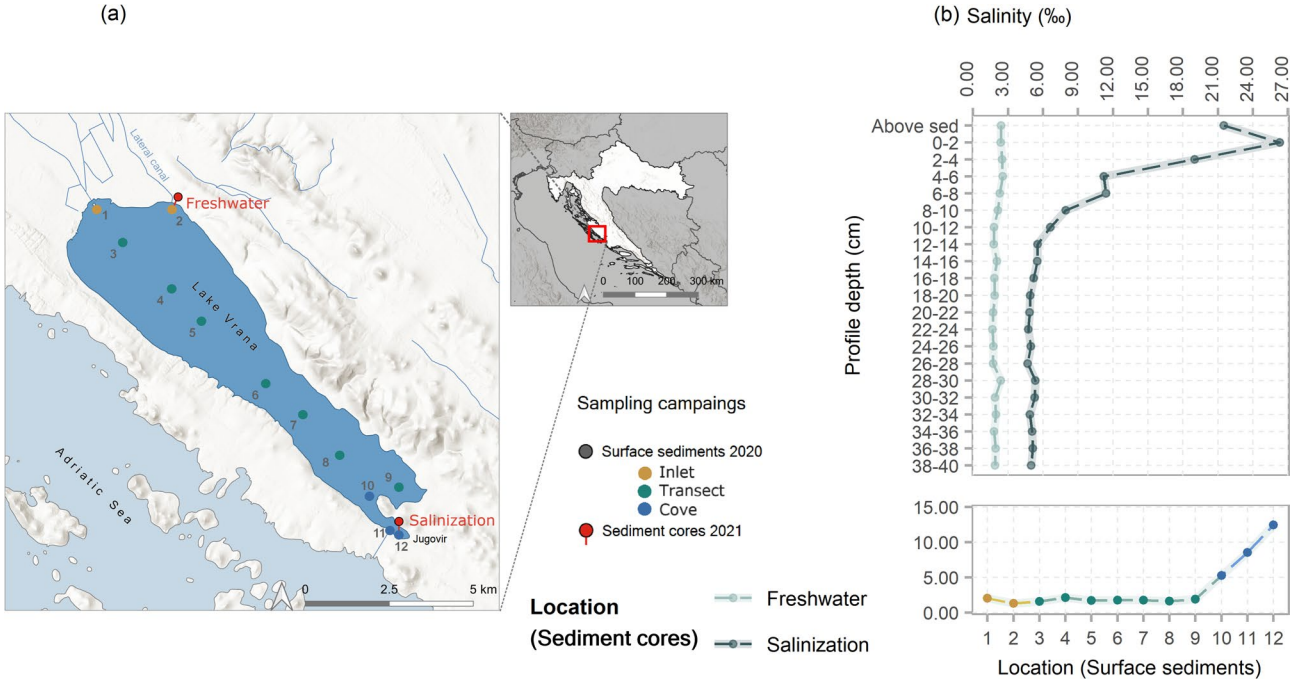

Fig. 1 (**a**) Map of Lake Vrana containing specific lake zones and annotated sampling campaigns with associated sampling stations. (**b**) Lake salinity measurements in sediment core profile and surface sediments

Methods

Sampling campaigns

Two sampling campaigns were conducted in Lake Vrana (Fig. 1a). In September 2020, surface sediment samples (top ~ 5 cm) were first collected to identify sites with the strongest microbial community-composition and salinity contrasts. These were collected with a Van-Veen grab sampler at twelve stations: inlet (1,2), with highest OM loading [33, 34], a transect (stations 3–9), and the salinization-affected cove (stations 10–12) where the underwater conduit links the lake to the Adriatic Sea (Salinity ~ 38). Approximately 400 ml of surface sediment per station was collected and preserved on ice.

In September 2021, based on the findings from the initial surface sediment analysis and real-time water-column salinity monitoring, deeper sediment profiles (40 cm) were collected in triplicate from two locations: the salinization zone (Jugovir, station 12) and a freshwater zone (station 2). Samples were retrieved using a gravitational corer (UWITEC, USC 6000, Austria) and transported for geochemistry and microbial community analysis.

Sample preparation, physicochemical and molecular analyses

Upon arrival at the laboratory, surface sediment samples were centrifuged (SL 16 R, Thermo Fisher Scientific, MA, USA) to extract pore water. A 15 ml pore water aliquot was filtered (PTFE hydrophilic filter, IsoLab. GmbH, Eschau, Germany), and analyzed by ion chromatography (Dionex DC IC-1000/IC-1100, CA, USA) under following conditions: for anions: 8 mM $NaHCO_3$ and 1mM Na_2CO_3 eluent, column (Dionex IonPac AS14A, CA, USA) at room temperature, suppressor current at 43 mA, and 1.2 ml/min flow rate; for cations: 30 mM methanesulfonic acid eluent, column (Dionex IonPac CS16, CA, USA) at 40 °C, 88 mA suppressor current, and 1.2 ml/min flow rate. Salinity was measured with a handheld refractometer (PCE-0100, GmbH, Germany), confirmed by chloride-based salinity calculation. Sediment profile samples were sectioned into 2 cm layers, processed in a nitrogen-flushed glove bag (Captair Pyramid, Erlab, MA, USA), and transferred to Falcon tubes. After centrifugation, pore water was used for ion chromatography and dissolved methane measurements. Headspace dissolved methane concentrations were determined using a GC-FID system (Agilent 7890, Santa Clara, CA, USA) and calculated as described in [35], considering methane solubility coefficients under different salinities [36].

For DNA extraction, 0.5 g and 0.25 g of homogenized surface and profile sediment samples, respectively, were used. DNA extraction was performed with the DNeasy PowerSoil and PowerSoil Pro kits (Qiagen, Valencia, CA, USA). qPCR was performed on 12 surface sediment and 36 sediment profile DNA samples to quantify abundances of *pmoA* [37], *mcrA* [38], *dsrAB* [39], and the V4 region of the 16 S rRNA [40, 41] genes. Triplicate qPCR reactions were conducted for each sample, including

standards (10^7– 10^1 gene copies μL^{-1}) and negative controls on a Bio-Rad CFX96 system (Bio-Rad, CA, USA; detailed methods provided in Supplementary Protocol I).

Sequencing and bioinformatics analysis

The V4 hypervariable region of the 16 S rRNA gene of bacteria and archaea was amplified using 515 F [40] and 806R [41] primers as described previously [42], and sequenced on the Illumina MiSeq (V3 chemistry, 600 cycles) at the Joint Microbiome Facility, Medical University of Vienna and University of Vienna (project ID JMF-2103-15). Further details on amplicon data processing are in Supplementary protocol II.

Based on qPCR, amplicon sequencing results and physicochemical properties, fourteen sediment profile samples were selected for metagenomic sequencing (project ID JMF-2211-11), including samples located above, within, and below the unconventional SMTZ - characterized by incomplete sulfate depletion, non-continuous methane accumulation, and a distinct subsurface methane peak (Fig. 2c). Metagenomic read sets were trimmed, quality filtered, and normalized before *de novo* assembly using MEGAHIT (v. 1.2.9 [43]), and binning into metagenome-assembled genomes (MAGs) using MetaBAT2 [44]. MAGs were refined, dereplicated, and assessed for quality, with subsequent taxonomy assignment using GTDB-Tk (v. 2.1.1 [45]). Functional annotation focused on genes related to osmoregulation, multi-heme cytochromes, pili, and key metabolic pathways for methanogenesis, methanotrophy, and sulfate reduction. Detailed metagenome data analysis information including network analysis of MAGs is provided in Supplementary protocol III.

Statistical analysis

Statistical analysis of qPCR results was performed in R (v. 4.3.1 [46]). ANOVA test with a post-hoc Tukey test was applied for normally distributed datasets, and Kruskal-Wallis, and Wilcoxon test for non-normally distributed datasets, to test for significance in differences of gene copy numbers and in environmental parameters between specific geographic locations (inlet, transect, cove) of surface sediments. Sediment profile qPCR results were reported as relative abundances (functional gene copy numbers normalized to total 16 S rRNA gene copy numbers), while surface sediment results also included gene ratios.

Representative reads related to methanogens, aerobic methanotrophs, ANME, and SRB were subsampled based on assigned taxonomy from the 16 S rRNA gene datasets. Alpha diversity (Shannon index [47] and species richness) was calculated on rarefied datasets. PERMANOVA was used to explore correlations between microbial communities and physicochemical parameters

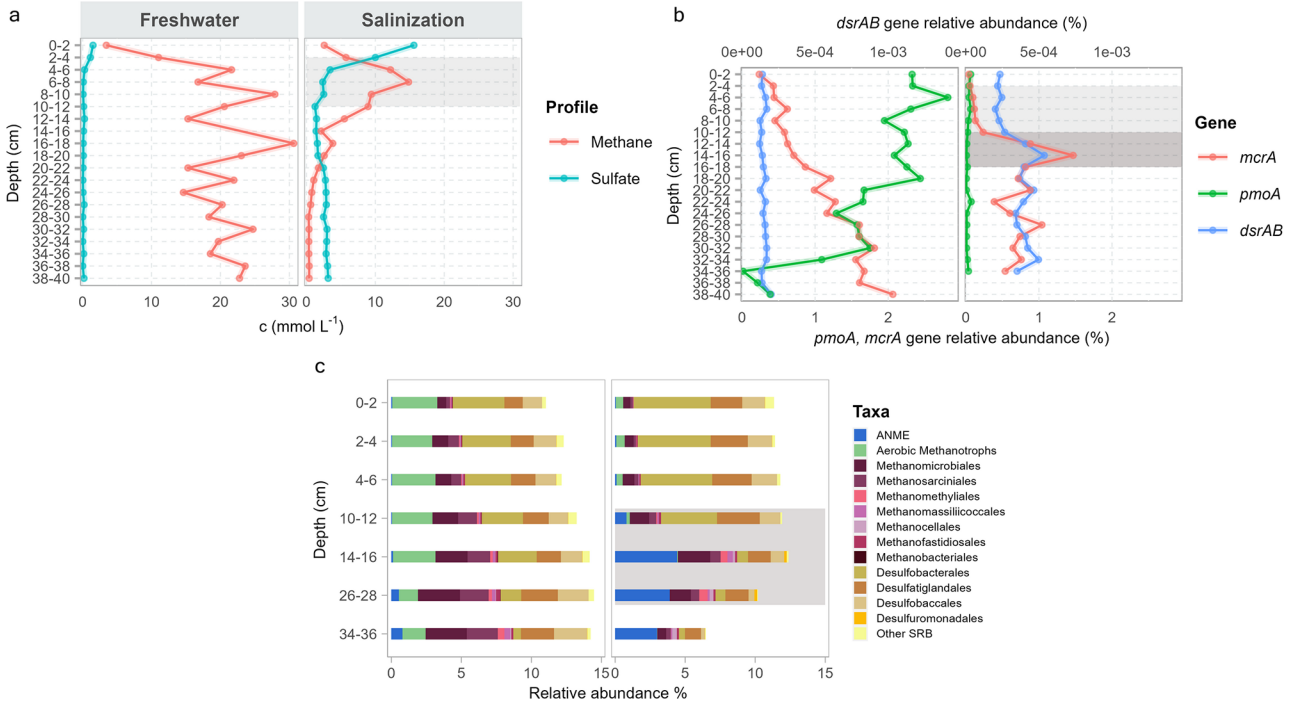

Fig. 2 (**a**) Depth profiles of sulfate and methane concentrations in sediments. The SMTZ is highlighted. (**b**) Relative abundances of functional gene copy numbers involved in the methane cycle, retrieved from sediment profiles at freshwater and salinization stations, normalized by the 16 S rRNA gene copy numbers. Light grey-SMTZ, dark grey-*mcrA* and *dsrAB* peak (**c**) Relative abundances of methanogens, methanotrophs, and SRB communities in sediment profiles, based on 16 S rRNA gene sequence data derived from metagenomes. ANME peak relative abundance is highlighted in grey

using Bray–Curtis dissimilarity matrices [48]. Principal Coordinates Analysis (PCoA) was applied to assess microbial community dissimilarities across sediment profiles for each selected functional group, with significant physicochemical parameters overlaid as vectors on the PCoA plots. Differential abundance analysis was performed on ASV level, on the 16 S rRNA gene amplicon data from sediment profiles using DESeq2 [49]. Log fold changes were computed for centered log-ratio clr transformed relative abundance data from freshwater samples relative to salinized sediments, and a Benjamini-Hochberg adjusted p-value threshold was set at 0.05. After calculation of differential abundance, all significantly differentially abundant ASVs belonging to the same sulfate-reducing or methane-cycling taxa at genus, family, or order level were clustered to compute mean log fold change values for the respective taxon. ASVs with read count number less than a 100 in at least one sample, and with a total relative abundance below 0.5% across the entire community were excluded prior to clustering and averaging. Differential MAG abundance was assessed using a Wilcoxon rank-sum test on clr transformed abundance data between the salinization and freshwater sites. P-values were adjusted for multiple comparisons with the Benjamini-Hochberg method, and significance was set at a threshold of 0.05.

Results

Geochemical characterization of lake sediments

Surface sediment pore water salinity significantly varied between the cove and the rest of the lake (ANOVA, Tukey, $p < 0.001$). Salinity and sulfate concentrations peaked in the cove, with station 12 exhibiting the highest values (Fig. 1b, Supplementary Fig. S1c). The salinization sediment profile, at all depths, had higher salinity (26.3–4.7‰) than the freshwater sediment profile (2.5–1.7‰, Fig. 1b). Sulfate concentrations were on average four times higher in the salinization profile and decreased with depth in both profiles (Fig. 2a). While sulfate was depleted at ~10 cm depth in the freshwater profile, elevated sulfate concentrations remained throughout the salinization sediment profile with a minimum of ~2 mmol L^{-1} at 10–20 cm (Fig. 2a). Freshwater methane concentrations sharply increased from the surface to 4–6 cm depth, likely reflecting an upward diffusion gradient, and thereafter fluctuated at high concentrations (~20 mmol L^{-1}, Fig. 2a). Methane concentrations were lower in the salinization profile, peaking at 6–8 cm sediment depth (14.8 mmol L^{-1}), thereafter, decreasing with depth (Fig. 2a). Notably, no "classical" SMTZ formed, where sulfate is depleted with depth and methane is accumulating. Instead, sulfate remained present throughout the salinization profile (Fig. 2a).

Spatial and depth distribution and diversity of methane cycling microorganisms in lake sediments

In surface sediments, normalized *pmoA* and *mcrA* gene abundances ranged from 0.3 to 2.7% and 0.1–1.9%, respectively, with both being lowest in the cove (Fig. S2a, S2b). The inlet had the highest *pmoA* abundance and the lowest *mcrA/pmoA* ratio (Supplementary Fig. S2d). The *pmoA* and *mcrA* gene abundances positively correlated across the transect (Supplementary Table S1a), while *dsrAB* abundance increased from inlets to the cove (Supplementary Fig. S2c). The *mcrA*/*dsrAB* ratio was highest at the inlet but lowest in the cove (Supplementary Fig. S2e). 16 S rRNA gene-based community composition and diversity of methanotrophs and SRB varied spatially, with increasing dissimilarity from inlet to cove (Supplementary Results; Supplementary Table S3, Supplementary Fig. S4).

In sediment depth profiles, *pmoA* gene abundances were significantly higher throughout the freshwater profile compared to the salinization profile (Fig. 2b). Relative *mcrA* gene abundances were also higher in freshwater, increasing continuously with depth, whereas in the salinization profile, *mcrA* was nearly absent in the top 10 cm before stabilizing at higher abundance at greater depths (Fig. 2b). *dsrAB* gene abundance was higher in the salinization profile. A robust positive correlation between *dsrAB* and *mcrA* gene abundances and a negative correlation between *dsrAB* and methane concentrations were observed in the salinization profile (Fig. 2b, Table S1b), while there were no such correlations in the freshwater profile.

In surface sediments of the inlet, ANME proportions decreased, while bacterial aerobic methanotrophs increased (1–4) (Supplementary Figs. S2, S4). Methanogen composition remained stable across the transect (Supplementary Fig. S4), whereas SRB composition was more spatially homogeneous, except for SEEP– SRB1, which increased toward the cove and peaked at the salinization station (station 12, Supplementary Fig. S4).

Methanogenic communities were similar across the freshwater profile, but distinct with depth in the salinization profile (Supplementary Fig. S6b). Methanotrophic communities in the salinization profile are separated into upper (up to 6 cm) and deeper (10–36 cm) layers, while in the freshwater profile, only the deepest samples clustered separately (Supplementary Fig. S6b). The SRB exhibited higher dissimilarity between profiles in the deeper sediment layers, which clustered separately from the surface communities of both profiles (Supplementary Fig. S6b). The 16 S rRNA gene-based diversity and community composition of all three functional groups significantly correlated with dissolved methane concentrations (PERMANOVA, $p < 0.05$), and each functional group differed significantly between the two profiles

(PERMANOVA, $p < 0.05$). Methanogen alpha diversity increased with depth in both sediment profiles (Supplementary Fig. S6a), despite lower relative abundances in the salinization profile (mean 2.0% vs. 3.4% in freshwater). Methanogen community composition differed significantly in deeper sediment layers. Methanomicrobiales dominated the salinization, and Methanosarcinales and Methanomicrobiales prevailed in the freshwater profile (Fig. 2c). Methanotroph and SRB alpha diversity peaked in upper layers (up to 6 cm), followed by a pronounced decline with depth in the salinization profile (Supplementary Fig. S6). There, SRB had an overall higher relative abundance up to 10–12 cm, decreasing below, accompanied by the occurrence of groups exclusively present in deeper zones of salinization (14–16 cm, 26–28 cm), such as Desulfomonadales and Desulfomaculales (Supplementary Fig. S7). The SRB displayed a comparatively homogeneous community composition and abundance distribution in the freshwater profile, except for the lower relative abundance of the Desulfobacterales in deepest samples (26–28, 34–36 cm). Aerobic methanotrophs were less abundant and completely replaced by ANME-1 at sediment depths > 10 cm in the salinization profile (Fig. 2c). In the freshwater profile, aerobic methanotrophs were abundant at all depths, with ANME-1 only showing increased relative abundances in the deepest layers (> 26 cm) (Fig. 2c). The distinct spatial distributions along the sediment profiles were confirmed by differential abundance analysis, with 10 sulfate-reducing and methane-cycling taxa, including all ANME clades, being statistically significantly less abundant in freshwater sediments (Fig. 3a). In contrast, 18 taxa were significantly more abundant in freshwater sediments (Fig. 3a), comprising mostly methanogens and aerobic methanotrophs, and 2 SRB-lineages (*Desulfomonile*, *Desulfobacca*).

Amongst these significantly differentially abundant sulfate-reducing and methane-cycling microorganisms, nine clades accounted for a relative abundance of more than 0.5% across the sediment profiles, and were thus inspected in more detail. Three out of 5 detected ANME-1 were enriched in the salinisation profile (Fig. 3b). These were accompanied by three enriched SEEP-SRB1 ASVs, which were relatively more abundant at depths of the SMTZ in salinized sediments, and two *Desulfatiglans*-affiliated ASVs found to be more abundant below the SMTZ in salinized sediments. In the freshwater sediment profile, two ASVs related with aerobic methanotrophs and two ASVs affiliated with the methanogens *Methanoregula* and *Methanosaeta* were significantly more abundant than in the salinisation profile. Within the freshwater profile. as expected, methanotroph ASV relative abundances were declining with depth, while the methanogen ASVs increased in relative abundance with depth (Fig. 3b).

Comparative genomic insights into microbial communities between the freshwater and salinization-impacted sediment profile

To investigate genomic adaptations to salinization, metagenomes were sequenced from 14 samples, representing 7 different depths of each sediment profile. Assembly and binning of the metagenomic data yielded 221 MAGs with completeness > 50% and contamination < 10% (Table S4.). Among these, we recovered 38 SRB MAGs containing *dsrAB* genes (Desulfobacterota phylum), including 6 Syntrophales MAGs lacking genes for dissimilatory sulfate reduction other than *dsrAB*. Notably, 13 SRB were uniquely present in the salinization, predominantly in deeper layers (marked with (*), Supplementary Fig. S8.), which were already observed to host a clearly distinct SRB community based on 16 S rRNA gene amplicon data (Fig. 2c., Fig. S7. in detail). Methanotrophs were represented by 6 MAGs carrying *mcrA* genes, all belonging to the ANME-1 (ANME-1-THS, QENH01, and JACGMN01 genera), and 2 aerobic methanotroph MAGs encoding *pmoA* (Methylobacter_01, Methylococcaceae_01) (Supplementary Fig. S9). ANME-1 MAGs were most abundant in deeper layers of the salinization (Fig. S9), while aerobic methanotrophs were prevalent in the freshwater profile (Supplementary Fig. S9). Methanogens, identified by the presence of *mcrA* genes, were represented by 12 MAGs in five orders, predominantly in the deeper layers of the freshwater profile. The complete methanogenesis pathway was only present in the Methanotrichaceae_01 MAG (93.59% genome completeness; Supplementary Fig. S10).

In total, 24% of the MAGs were differentially abundant between the salinization and freshwater sediment profile with 7% connected to the salinization (Fig. 4a, c). There were no differences in the genome size of site-specific MAGs, while MAGs most abundant in the deepest layers of the salinization profile had the smallest genomes within that profile. Likewise, there were no differences in the salinization-induced distribution of genes for different osmoregulation strategies in differentially abundant MAGs (Fig. 4a, c).

Genes related to osmoregulation were further explored in the above-described selected MAGs (Fig. 4c.) to assess if the methane and sulfur cycling microorganisms display specific adaptations to increased salinity. We examined the following osmoadaptation mechanisms: efflux pumps, transport systems, osmoprotectant biosynthesis, porin synthesis, protein secretion, and genes encoding cell stress response. The gene encoding aquaporin Z (*aqpZ*), enhancing and regulating water transfer from and into the cell, was present in half of the recovered SRB MAGs. However, it was not more frequent in MAGs overrepresented in the salinization profile. Accumulating osmolytes or compatible solutes is another way to

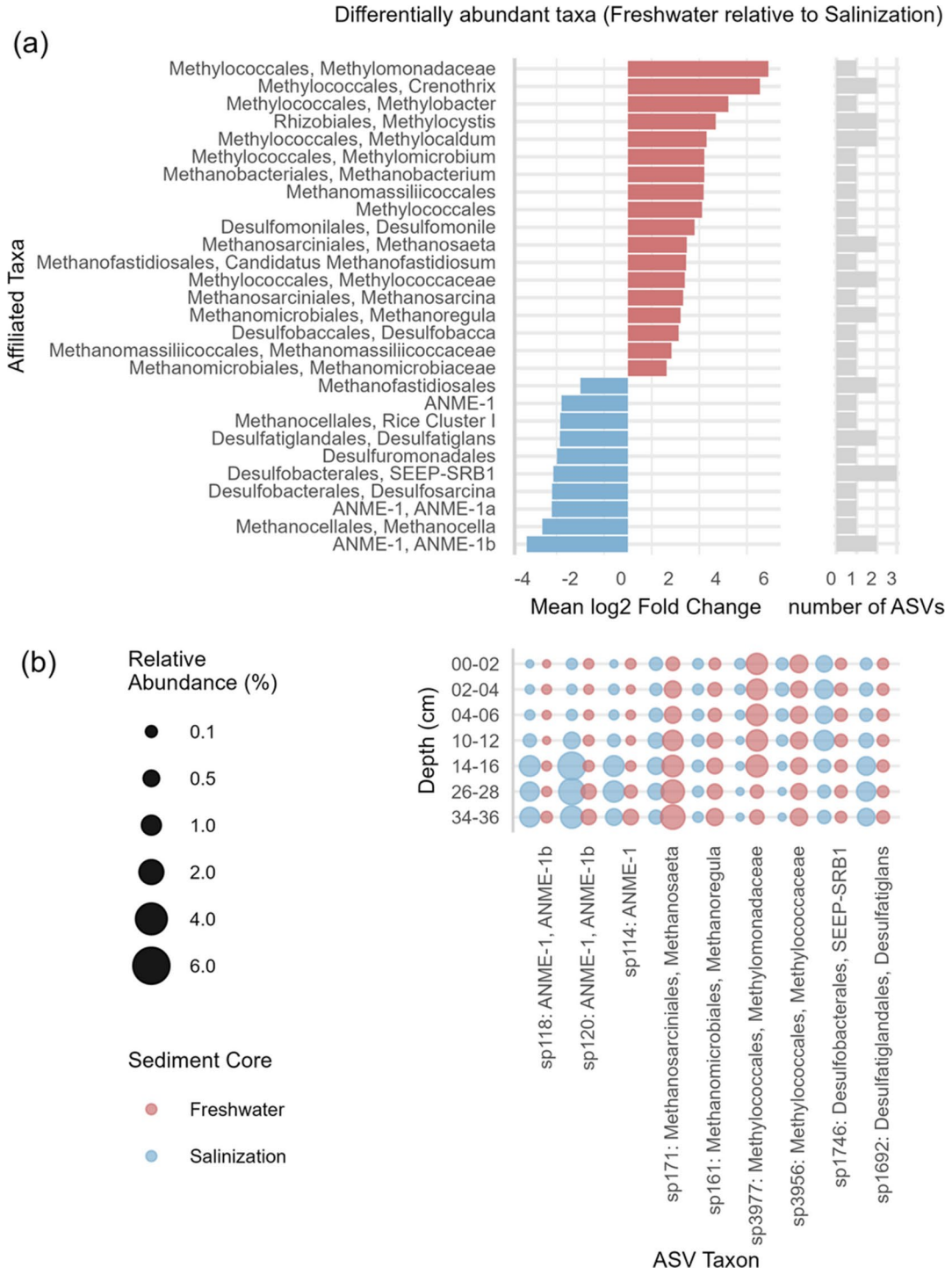

Fig. 3 (**a**) Differentially abundant taxa represented by the mean log2 fold change in the freshwater sediment depth profile relative to the salinization profile (*padj.* < 0.05). Bars indicate taxa depleted (blue) or enriched (red) in freshwater compared to salinized sediments. The number of distinct ASVs affiliated with each taxon is shown in grey. The y-axis shows the lowest assigned taxonomic level for each group. (**b**) Relative abundance of differentially abundant ASVs (count number > 100, relative abundance > 0.5%) along depth profiles of salinization and freshwater sediment cores. ASV identifiers (sp-N) are labeled alongside their affiliated taxonomy

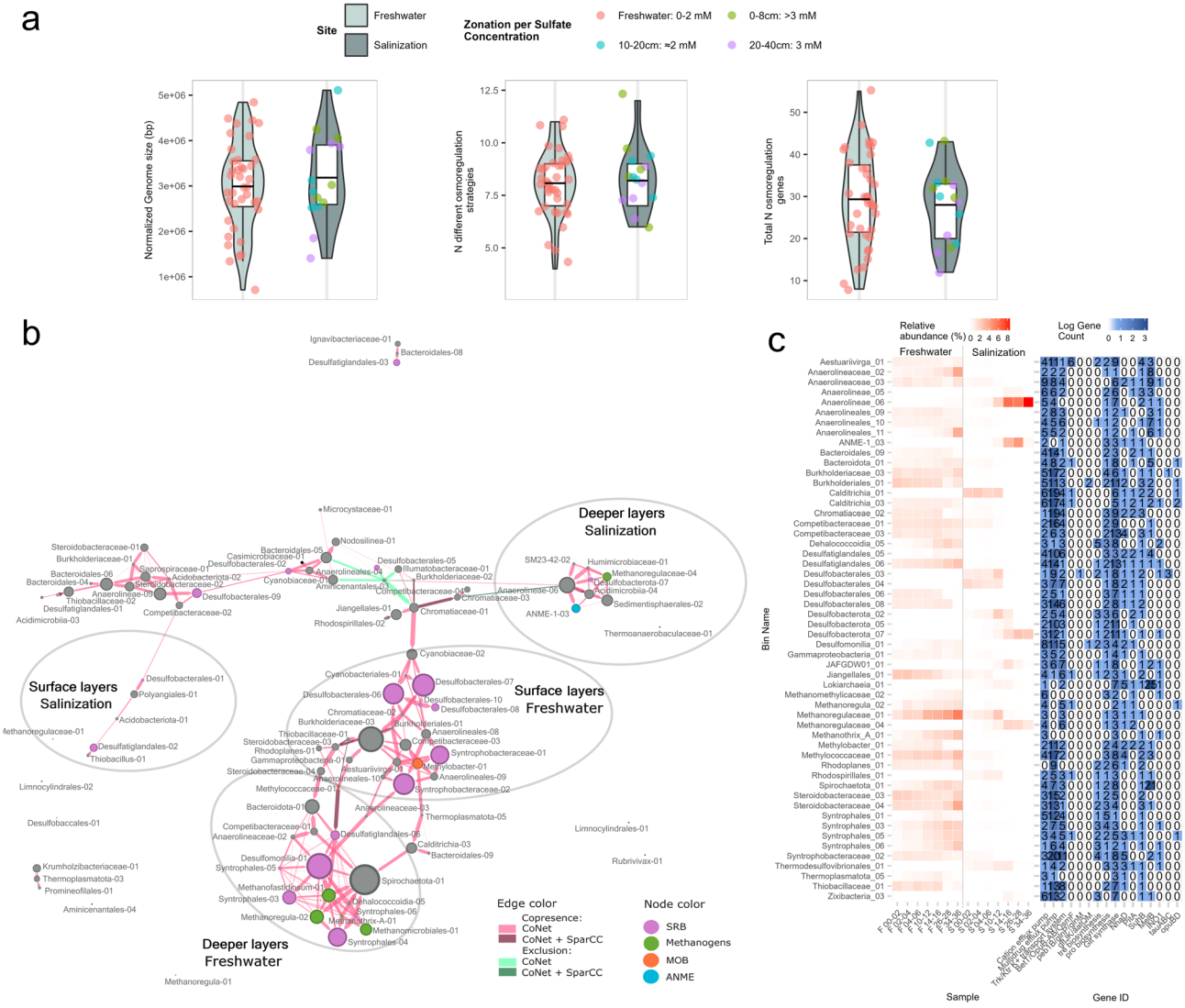

Fig. 4 (**a**) Statistical values of differentially abundant MAGs between freshwater and salinization samples, showing genome size (normalized by genome completeness), number of different osmoregulation strategies, and cumulative number of osmoregulation genes present in genomes. Individual genomes are colored according to the sulfate concentrations in the environment where they are most abundant. Mean values are represented by a line. (**b**) Co-occurrence network analysis of MAGs (completeness > 50, contamination < 10), calculated with CoNet and SparCC, highlighting microbial genomes involved in the methane cycle. Node color indicates functional group, node size reflects the number of correlations, edge color represents the type of correlation, and edge size is weighted by correlation strength. The assigned taxonomy for each MAG is added to corresponding nodes and modularity clusters of interest are encircled. (**c**) Differential relative abundance of MAGs in freshwater and salinization sediment profiles, along with their affiliated osmoregulation gene content

regulate cellular osmolarity at elevated salinity. Proline biosynthesis genes were present in nearly all SRB MAGs. Trehalose biosynthesis genes were also prevalent, occurring in MAGs abundant in both sediment profiles (Supplementary Fig. S8). Genes related to glycine-betaine synthesis were present in nine SRB MAGs. Ectoine biosynthesis genes were only present in the Syntrophobacteria_01 MAG. Amongst the methanotrophs, all ANME MAGs contained the CHDH gene involved in glycine-betaine biosynthesis and a complete pathway for proline synthesis. The ANME-1_02 MAG additionally contained genes encoding aquaporins, as well as the *dnaK* and *groEL* genes (Supplementary Fig. S9). The methanogen MAG Methanofastidiosum_01 contained the highest number of genes involved in osmoregulation via osmoprotectant generation, despite occurring predominantly in the freshwater profile (Supplementary Fig. S9). Aerobic methanotroph MAGs contained the least diverse set of genes associated with adaptation to high osmolarity (Fig. S9). No clear relation was observed between MAG relative abundance in the two profiles and increased osmoregulation-related gene diversity (Fig. 4a, c).

In ANME and SRB MAGs, genes encoding MHC and pili, indicative of the potential for extracellular e-transfer important in syntrophic partnerships, were also examined. The *qrcA* gene encoding menaquinone reductase, associated with sulfate respiration and extracellular e-transfer, was found in Desulfobacterales and Desulfatiglandales orders (Desulfatiglandales_04, Desulfobacteria_01 and 02) (Supplementary Fig. S8). All SRB MAGs contained heme–binding motifs ($CX_{(n2-5)}CH$), with 8 predicted as extracellular in bins Desulfomonilia_01 (quantity: 1, genus MWEI01), Desulfobacteria_02 (quantity: 2, genus C00003060), Desulfatiglandales_04 (quantity: 2, genus B33-G16), and Dissulfuribacterales_02 (quantity: 3, genus UBA3076) (Table S5). Type IV pilus genes (*pilABC*) were present in all SRB MAGs, except those affiliated with Desulfobacterales and Dissulfuribacterales. These genes were also identified in some ANME, methanogen, and aerobic methanotroph MAGs (Supplementary Fig. S9), with the QENH01 MAG ANME-1_02 having the highest number. In the same ANME-1_02 MAG, the most MHC gene copies were detected, and it was the only ANME MAG with heme-binding motifs, but no clear cellular localization predictions (Supplementary Table S5). There were no hydrogenases detected in methanogen, methanotroph, and SRB MAGs with a 50% identity cut-off.

We further performed a co-occurrence network analysis to investigate interactions between the recovered MAGs. The network contained 98 nodes and 202 edges, with only 5% correlations confirmed with both network inference approaches (Fig. 4b.). The network contained five site-specific clusters with the biggest belonging to the freshwater cluster and two smallest belonging to the salinization cluster. The only MAG in the network performing AOM was ANME-1-03, which co-occurred with Anaerolinae-06 and Acimidimicrobiia-04, while being in the same salinization cluster as Desulfobacterota-07 and Methanoregulaceae-04 MAG.

Discussion

Changes in sediment geochemistry induced by salinization affect microbial communities involved in methane cycling

Geochemical analysis of surface sediments and sediment profiles highlights stark biogeochemical differences between freshwater and salinized sediments of Lake Vrana. Salinization leads to elevated sulfate concentrations both above and below a methane pocket which forms near the surface of salinized sediments (Fig. 2). The geochemical and microbiological profile around this pocket resembles an SMTZ, uncommon in freshwater [50] but typical in marine environments [21]. Unlike conventional SMTZ dynamics, where sulfate depletes with increasing methane at depth, our study shows a peak in methane concentration followed by its depletion, while sulfate levels remain relatively unchanged and even again increase with depth (Fig. 2a). Previous studies linked brackish water with reduced methane emissions from coastal fens [31] and peatlands [51] by lowering the SMTZ depth via salinization. Our findings suggest a unique impact of salinization on methane dynamics, diverging from patterns observed in permanently saline sediments [52]. Uncertainties remain regarding sulfate and methane profile variability, including the impact of the frequency of salinization events and sulfate diffusion fluxes. The non-steady state profiles observed in the salinized zone suggest two-directional sulfate diffusion within these sediments: downward diffusion from the salinized water column and upward or lateral diffusion through deeper sediment layers due to density differences between fresh and saline waters (Fig. 2a). This particular geochemical setting promotes sulfate-dependent AOM and reshapes methane dynamics.

Microbial functional guild distribution varied notably with salinity. The absence of aerobic methanotrophs in salinized sediments, particularly at depths greater than 12 cm (Fig. 2b, 2), aligns with a prior study [29] reporting a decline in aerobic methanotrophs due to higher salinity. However, the observed changes in the distribution of aerobic methanotrophs are likely not driven only by salinity but also by the spatial heterogeneity of OM quality and quantity, as well as different sedimentation rates (~2.5 mm/yr) between inlet (6.4 mm/yr) and cove sites [53]. The occurrence of sulfate-dependent AOM and ANME-SRB syntrophy [54] in salinized sediments (Fig. 2b, c, and 3a), in particular at depths where methanogen populations are declining (Fig. 2c), is a novel finding from our study. While *mcrA* gene copy numbers may in parts reflect presence of dormant methanogens and can't directly be linked to activity, the negative correlation between *mcrA* gene abundance and methane concentrations in the salinized zone points to an increase in ANME, rather than methanogens (Supplementary Table S1b), contributing to this pattern. Future studies using qRT-PCR could confirm the active portion of the methanogenic population. Yet, while sulfate-dependent AOM contributes to methane oxidation throughout the entire anoxic salinized sediment, the lack of aerobic methanotrophs at shallow depths possibly allows a fraction of methane to escape oxidation. At the lake inlets, allochthonous OM input from tributaries [34] and the low sulfate concentrations create favorable conditions for methanogenesis at shallow depths [55, 56], resulting in sediment oversaturation with methane. Aerobic methanotrophs are abundant in the freshwater sediment profile, with only a slight decrease in abundance with depth (Fig. 2b, c). Their abundance at higher sediment depths does not necessarily reflect an active aerobic methanotrophic community, as oxygen penetration in sediments

of eutrophic lakes rarely excites the top few micrometers [57]. It is possibly a reflection of biomass burial due to high sedimentation rates at inlets [53]. Similar observations of aerobic methanotrophs in anoxic layers, even in lakes with lower sedimentation rates (2.8 cm/yr) have also been reported [58, 59], and activity of aerobic methanotrophs in anoxic lake waters has recently been shown [60 and references within]. While the exact reasons for the high abundance of aerobic methanotrophs in deeper sediment layers at the inlet warrant further investigation, the sedimentary methane profile (Fig. 2a) shows that methane production exceeded methane consumption in these layers.

Similarly, both methanogen and SRB communities exhibited spatial heterogeneity between sediment profiles. While some SRB engage in syntrophic partnerships with ANME or methanogens, others compete with methanogens [18, 59]. In the salinized zone, methanogen abundance peaked at 14–16 cm, coinciding with a leveling off of sulfate concentration, SRB abundance, and salinity. A decrease in sulfate concentration and SRB relative abundance, particularly the Sva0081 group, was observed (Supplementary Fig. S7). These shifts are likely driven by changes in sulfate concentration and OM availability [60], shaping distinct SRB communities. The SEEP-SRB1 group, associated with ANME syntrophy in marine environments [61], was abundant in the salinized zone, but surprisingly did not co-vary with ANME populations (Supplementary Fig. S7). In the freshwater zone, enriched with organics and nutrients [34], SRB abundance was low and remained stable, while methanogen abundance increased with depth. Hydrogenotrophic (Methanoregulaceae) [62], methylotrophic (Methanomassiliicoccales, *Candidatus Methanomethylicus*, *Methanofastidiosum*), and acetoclastic methanogens (*Methanosaeta* and *Methanosarcina*) [63] were all present throughout the freshwater profile, with no significant shifts with depth (Fig. 2a, Supplementary Fig. S7). However, acetoclastic methanogens were less abundant in the saline sediments, likely due to competition with the acetate-utilizing Sva0081 group [64] (Supplementary Fig. S7).

Co-occurrence network and genomic potential analysis reveal interactions between sedimentary microorganisms during salinization

Co-occurrence network analysis was used to gain insights into microbe-microbe interactions [65] and revealed five clusters of interacting MAGs structured around methanogen, methanotroph, and SRB interactions within the broader microbial community. The largest cluster contained freshwater sediment-derived MAGs from taxa known to be involved in OM decomposition, which aligns with the OM-rich environment of this zone. Here, syntrophic SRB, affiliated with Syntrophobacteraceae in the shallow freshwater subcluster and Syntrophales in the deeper freshwater subcluster, were prevalent. The positive co-occurrence of various Syntrophales MAGs, known to oxidize fatty acids, with *Methanoregula* and *Methanothrix* MAGs suggest the occurrence of C2-C4 syntrophic metabolism between SRB and methanogens as suggested for bioreactors [66], or potential DIET as recently hypothesized for freshwater lake sediments [67].

The geochemical zonation of freshwater sediments with low sulfate concentrations in shallow layers and higher environmental adaptability of SRB compared to methanogens shapes the microbial community structure. In particular, the competition for hydrogen and acetate in the shallow freshwater subcluster helps define the separation of SRB in the shallow freshwater zone and methanogens in the deeper subcluster. Both clusters contain heterotrophic OM degraders such as Anaerolineaceae, Spirochaetota, and Bacteroidales [68, 69]. The only MAG affiliated with MOB was found in the surface freshwater subcluster, likely due to its sensitivity to osmotic pressure (Supplementary Fig. S9). MAGs from deeper saline layers exhibited co-occurrence of anoxic metabolisms, including halophilic anoxic Sedimentisphaerales, Anaerolineae, Desulfobacterota, ANME-1, and Methanoregulaceae, which support the oxidation of a range of complex to simple carbon compounds under saline conditions [70, 71]. Their separation from MAGs of the surface layer-salinized subcluster (Fig. 4b) highlights the clear community shift above and below the methane pocket in salinized sediment.

The wide spatial distribution and abundance of SRB underscore their pivotal role in shaping methanogenic and AOM communities, especially in the salinized zone (Fig. S8). Our observations align with studies showing that SRB outcompete methanogens under conditions of higher sulfate and lower OM availability, as is commonly observed in marine sediments [58, 72]. However, another role of certain SRBs in the methane cycle is their ability to form associations with ANME. The functional genomic potential of specific SRB taxa, such as SEEP-SRB1 that encodes large MHC and type IV pili, facilitating extracellular e-transfer [58], indicates their involvement in AOM. We found several *Desulfobacterota* MAGs, including SEEP-SRB1c and SEEP-SRB2 [73], encoding the type IV pili synthesis pathway and/or multiple extracellular MHCs, indicative of the potential for DIET [74]. SEEP-SRB2 MAGs were abundant in deeper layers of the salinization profile, alongside ANME-1 (Supplementary Fig. S8, S9), further supporting their involvement in AOM syntrophy [15, 73]. Lastly, SEEP-SRB1 genomes syntrophic with ANME contain MHCs but lack periplasmic hydrogenase and formate dehydrogenase genes, unlike those occurring outside the consortia [75] - a distinction also evident in the genome analysis within our study,

further confirming their engagement in syntrophy during salinization.

Genomic potential for osmoregulation mechanisms for adaptations to increased salinity

Salinization-induced shifts in microbial communities involved in sulfur and methane cycles, observed at a depth of 14–16 cm, align with a reported salinity threshold of 5‰ [76]. Halophilic and halotolerant microorganisms adapt through mechanisms like aquaporins, compatible solutes, cell wall modifications, osmosensing mechanisms, signal transduction, ion transport systems, and stress response pathways [77, 78]. As a result of long-term salinity pressure, the selection of different genome sizes of bacteria and archaea has been reported, with bacteria exhibiting reduced genomes while archaea contained larger genomes and more salt-resistance genes [79]. Here, interestingly, microorganisms differentially abundant in saline versus freshwater sediments did not show significant differences in genome sizes or genomic potential for osmoregulation. Many MAGs, independent of their preference for saline or freshwater sediments, harbored the genomic potential for adapting to increased salinity by encoding osmoprotectants such as trehalose, ectoine, and proline, as well as genes for protecting cellular structures and enzymes from osmotic stress (e.g., *dnaK*, *groEL*). Proline synthesis genes were found in all differentially abundant microorganisms (Fig. 4c.), including three functional groups involved in the microbial methane cycle (Supplementary Fig. S8, S9). Proline does not only serve osmotic regulation [80] but also plays essential roles in redox signaling and cell growth [81], which may explain its prevalence. Notably, the genomic potential for resilience against higher osmolarity was shown to be the lowest in aerobic methanotrophs, which could partially explain their absence in the salinization-impacted sediments (Supplementary Fig. S9). Likewise, the SRB exhibited the most extensive array of osmoregulatory genes, contributing to their robustness across both freshwater and salinized zones. However, no correlation was observed between the presence or copy number of genes related to osmotic stress resistance and the abundance or distribution patterns of examined MAGs in salinized versus freshwater sediments. Previous research has shown that microorganisms often exhibit resilience to short-term salinity changes in sediments [82]. Relatively moderate differences in sodium and chloride concentrations in this study, compared to truly hypersaline environments [83–85], as well as the transient nature of salinization, may account for the limited differences in osmotic stress adaptation potential between the investigated MAGs. The saline conditions occurring in Lake Vrana do not seem to be extreme enough to induce a selection for a distinct genomic potential with respect to osmotic stress. Instead, stress caused by seasonal salinization is likely mitigated at the level of differential utilization of the same genomic potential. An analysis of microbial activity using metatranscriptomics or metaproteomics could provide further insights. Metatranscriptomic analysis was attempted but RNA extraction from the sediment profile samples was not successful.

Conclusions

In conclusion, our findings suggest that while increased salinity can act as a stressor capable of altering community structure, it is not the primary driver of shifts between freshwater and salinized methane-cycling communities in Lake Vrana. Rather, the availability of sulfate as an electron acceptor creates a niche for SRB, particularly those forming consortia with ANME-1, and the rise in sulfate concentrations during salinization plays a pivotal role in the restructuring of sedimentary microbial communities. At the genomic level, no significant differences were observed between freshwater and salinized genomes with regard to osmoregulation, suggesting that seasonal salinization is insufficient to induce adaptations or selection on a genomic level. These insights enhance our understanding of methane cycle dynamics and the broader impacts of climate change-induced salinization on microbial processes and greenhouse gas emissions.

Abbreviations

ANME	Anaerobic methanotrophs
DIET	Direct interspecies electron transfer
MHC	Multiheme c-type cytochromes
AOM	Anaerobic oxidation of methane
SRB	Sulfate-reducing bacteria
SMTZ	Sulfate-methane transition zone
OM	Organic matter
MAGs	Metagenome-assembled genomes
PCoA	Principal coordinates analysis
aqpZ	Aquaporin Z gene
pilABC	Type IV pilus genes

Supplementary Information

The online version contains supplementary material available at https://doi.org/10.1186/s40793-025-00739-w.

Supplementary Material 1

Supplementary Material 2

Supplementary Material 3

Acknowledgements

We express our gratitude to the management of the Nature Park Vransko Jezero for their assistance during the fieldwork. Special thanks go to Dr. Neven Cukrov and his team for their guidance during sampling, and to Dr. Nives Matijaković Mlinarić and Martina Šparica Miko for their help in preparing the samples. We would also like to acknowledge Julia Ramesmayer and Jasmin Schwarz for sample processing in the JMF laboratories (Medical University of Vienna and University of Vienna), and Margarete Watzka and Andreas Richter for GC measurements at the University of Vienna.

Author contributions
L.S. contributed to the conceptualization of the study, including research design, hypothesis/aims formulation, and research supervision. She was involved in the methodology performing q-PCR, sample preparation, pore water and DNA extraction, physicochemical parameters measurements, and fieldwork. Her contributions also included investigation through metagenome and amplicon sequence processing, statistical data analysis, data visualization, drafting the original manuscript, and securing funding. D.V.M. provided supervision during the analysis and bioinformatics processing of metagenomic data. He also contributed to metagenome processing methodology and assisted with reviewing and editing the manuscript. M.M. contributed to the methodology, focusing on q-PCR. A.Č. and K.K. were involved in the methodology, specifically in fieldwork and pore water extraction. P.P. supervised the sample preparation for gas chromatography and contributed to the methodology including DNA extraction and sequencing. She also reviewed and edited the manuscript. S.O. provided research supervision throughout the research process, assisted with reviewing and editing, and secured research funding.

Funding
This study was funded by the Croatian Science Foundation under the projects DOK-2018-09-1550 and IP-2020-02-9021 (MALENA) and by the British Embassy Zagreb under the project "Insights into microbes involved in the methane cycle can help tackle climate change".

Data availability
The 16 S rRNA gene amplicon sequences from surface sediments are available in the Sequence Read Archive (PRJEB64649). Metagenomic sequencing reads of deeper sediment profiles are deposited under the Project ID PRJEB66120. MAGs generated in this study, along with supplementary data on MAG quality and taxonomy, are available on Figshare (10.6084/m9.figshare.25139249).

Declarations

Ethics approval and consent to participate
Not applicable.

Consent for publication
Not applicable.

Competing interests
The authors declare no competing interests.

Received: 24 February 2025 / Accepted: 6 June 2025
Published online: 17 June 2025

References

1. Johnson MS, Matthews E, Du J, Genovese V, Bastviken D. Methane emission from global lakes: new Spatiotemporal data and Observation-Driven modeling of methane dynamics indicates lower emissions. J Geophys Res Biogeosci. 2022;127(7):e2022JG006793.
2. Saunois M, et al. The global methane budget 2000–2017. Earth Syst Sci Data. 2020;12:1561–623.
3. Bastviken D. Methane. Encyclopedia of inland waters. Academic; 2009. pp. 783–805.
4. Praetzel LSE, et al. Organic matter and sediment properties determine in-lake variability of sediment CO2 and CH4 production and emissions of a small and shallow lake. Biogeosci. 2020;17:5057–78.
5. Liu Y, Whitman BV. Metabolic, phylogenetic, and ecological diversity of the methanogenic archaea. Ann. N Y Acad Sci. 2008;1125:171–89.
6. Peeters F, Encinas Fernandez J, Hofmann H. Sediment fluxes rather than oxic methanogenesis explain diffusive CH4 emissions from lakes and reservoirs. Sci Rep 2019; 9.
7. Reim A, Lüke C, Krause S, Pratscher J, Frenzel P. One millimetre makes the difference: high-resolution analysis of methane-oxidizing bacteria and their specific activity at the oxic-anoxic interface in a flooded paddy soil. ISME J. 2012;6:2128–39.
8. Oswald K, et al. Aerobic gammaproteobacterial methanotrophs mitigate methane emissions from oxic and anoxic lake waters. ASLO Limn Ocean. 2016;61:101–18.
9. Haroon M, et al. Anaerobic oxidation of methane coupled to nitrate reduction in a novel archaeal lineage. Nature. 2013;500:567–70.
10. Yin X, et al. Sulfate reduction and its important role in organic carbon mineralization in sediments of the Pearl river estuary. Estuar Coast Shelf Sci. 2021;206:107511.
11. Ouboter HT, et al. Methane-Dependent extracellular Electron transfer at the Bioanode by the anaerobic archaeal methanotroph candidatus methanoperedens. Front Microbiol. 2022;13:820989.
12. Orphan VJ, et al. Comparative analysis of methane-oxidizing archaea and sulfate-reducing bacteria in anoxic marine sediments. Appl Environ Microbiol. 2001;67:1922–34.
13. Kleindienst S, Ramette A, Amman R, Knittel K. Distribution and in situ abundance of sulfate-reducing bacteria in diverse marine hydrocarbon seep sediments. Environ Microbiol. 2012;14(10):2689–710.
14. Milucka J, Widdel F, Shima S. Immunological detection of enzymes for sulfate reduction in anaerobic methane-oxidizing consortia. Environ Microbiol. 2013;15:1561–71.
15. Segarra K, et al. High rates of anaerobic methane oxidation in freshwater wetlands reduce potential atmospheric methane emissions. Nat Commun. 2015;6:7477.
16. Zhao Q, Lu Y. Anaerobic oxidation of methane in terrestrial wetlands: the rate, identity and metabolism. STOTEN. 2023;902:166049.
17. Whitmare SL, Hamilton SK. Rapid removal of nitrate and sulfate in freshwater wetland sediments. J Environ Qual. 2005;34(6):2062–71.
18. Gomez Camacho CE, Rugerri B. Syntrophic microorganisms interactions in anaerobic digestion (Ad): a critical review in the light of increase energy production. Chem Eng Trans. 2018;64:391–6.
19. Paulo LM, Stams AJM, Sousa DZ. Methanogens, sulphate and heavy metals: a complex system. Rev Environ Sci Biotechnol. 2015;14:537–53.
20. Pester M, Knorr KH, Friedrich MW, Wagner M, Loy A. Sulfate-reducing microorganisms in wetlands - fameless actors in carbon cycling and climate change. Front Microbiol. 2012;3:72.
21. Borrel G, et al. Production and consumption of methane in freshwater lake ecosystems. Res Microbiol. 2011;162(9):832–47.
22. Deutzmann JS. Anaerobic methane oxidation in freshwater environments. In: anaerobic utilization of hydrocarbons, oils, and lipids: handbook of hydrocarbon and lipid microbiology. Cham: Springer 2020; 391–404.
23. Jeppesen E, Beklioglu M, Zadareev E. The effects of global climate change on water level and salinity: causes and effects. Water. 2023;15(15):2853.
24. Prusty P, Farooq SH. Understanding the effects of periodic freshening and salinization on coastal water quality and aquifer sediments through laboratory-based column experiments. J Hydrol. 2021;603:127060.
25. Herbert ER, et al. A global perspective on wetland salinization: ecological consequences of a growing threat to freshwater wetlands. Ecosphere. 2015;6(10):206.
26. Izabel-Shen D. Understanding response of microbial communities to saltwater intrusion through microcosms. CSBJ. 2021;19:929–33.
27. Luo M, Huang JF, Zhu WF, Tong C. Impacts of increasing salinity and inundation on rates and pathways of organic carbon mineralization in tidal wetlands: a review. Hydrobiologia. 2019;827:31–49.
28. Wood JM. Bacterial responses to osmotic challenges. J Gen Physiol. 2015;145(5):381–8.
29. Zhang S, et al. Salinity significantly affects methane oxidation and methanotrophic community in inner Mongolia lake sediments. Front Microbiol. 2023;13:1664–X302.
30. Rissanen AJ, et al. Effects of alternative electron acceptors on the activity and community structure of methane-producing and consuming microbes in the sediments of two shallow boreal lakes. FEMS Microbiol Ecol. 2017;93(7):fix078.
31. Gutekunst CN, et al. Effects of brackish water inflow on methane-cycling microbial communities in a freshwater rewetted coastal Fen. Biogeosciences. 2022;19(15):3625–48.
32. Frank J, Zhang X, Marcellin E, Yuan Z, Hu S. Salinity effect on an anaerobic methane- and ammonium-oxidising consortium: shifts in activity, morphology, osmoregulation and syntrophic relationship. Water Res. 2023;242:120090.
33. Selak L, Marković T, Pjevac P, Orlić S. Microbial marker for seawater intrusion in a coastal mediterranean shallow lake, lake vrana, Croatia. STOTEN. 2022;849:157859.

34. Selak L, et al. Adaptations of microbial communities and dissolved organics to seasonal pressures in mesotrophic coastal mediterranean lake. Environ Microbiol. 2022;24(5):2282–98.
35. Magen C, et al. A simple headspace equilibration method for measuring dissolved methane. Limnol Oceanogr Meth. 2014;12(9):637–50.
36. Wiesenberg DA, Guinasso NL. Equilibrium solubilities of methane, carbon monoxide, and hydrogen in water and sea water. J Chem Eng Data. 1979;24:356–60.
37. Kolb S, Knief C, Stubner S, Conrad R. Quantitative detection of methanotrophs in soil by novel pmoA-targeted real-time PCR assays. Appl Environ Microbiol. 2003;69(5):2423–9.
38. Steinberg LM, Regan JM. Phylogenetic comparison of the methanogenic communities from an acidic, oligotrophic Fen and an anaerobic digester treating municipal wastewater sludge. Appl Environ Microbiol. 2008;74(21):6663–71.
39. Leloup J, et al. Diversity and abundance of sulfate-reducing microorganisms in the sulfate and methane zones of a marine sediment, black sea. Environ Microbiol. 2007;9:131–42.
40. Parada AE, Needham DM, Fuhrman JA. Every base matters: assessing small subunit rRNA primers for marine microbiomes with mock communities, time series and global field samples. Environ Microbiol. 2015;18(5):1403–14.
41. Apprill A, McNally S, Parsons R, Weber L. Minor revision to V4 region SSU rRNA 806R gene primer greatly increases detection of SAR11 bacterioplankton. Aquat Microb Ecol. 2015;75(2):129–37.
42. Pjevac P, et al. An economical and flexible dual barcoding, two-step PCR approach for highly multiplexed amplicon sequencing. Front Microbiol. 2021;12:669776.
43. Li D, Liu CM, Luo R, Sadakane K, Lam TW. MEGAHIT: an ultra-fast single-node solution for large and complex metagenomics assembly via succinct de Bruijn graph. J Bioinform. 2015;31(10):1674–6.
44. Kang DD, et al. MetaBAT 2: an adaptive Binning algorithm for robust and efficient genome reconstruction from metagenome assemblies. Peer J. 2019;7:e7359.
45. Chaumeil PA, Mussig AJ, Hugenholtz P, Parks DH. GTDB-Tk: a toolkit to classify genomes with the genome taxonomy database. J Bioinform. 2020;36(6):1925–7.
46. R Core Team. R: A language and environment for statistical computing. R Foundation for Statistical Computing, Vienna, Austria. 2021. URL: https://www.R-project.org/
47. Shannon CE. A mathematical theory of communication. Bell Syst Tech J. 1948;27:623–56.
48. Bray JR, Curtis JT. An ordination of the upland forest communities of Southern Wisconsin. Ecology. 1957;38:325–49.
49. Love MI, Huber W, Anders S. Moderated Estimation of fold change and dispersion for RNA-seq data with DESeq2. Genome Biol. 2014;15(12):550. https://doi.org/10.1186/s13059-014-0550-8.
50. Kleint JF, Wellach Y, Schroll M, Keppler F, Isenbeck-Schröter M. The impact of seasonal sulfate–methane transition zones on methane cycling in a sulfate-enriched freshwater environment. ASLO Limnol Ocean. 2021;66(6):2290–308.
51. Pönisch DL, et al. Nutrient release and flux dynamics of CO2, CH4, and N2O in a coastal peatland driven by actively induced rewetting with brackish water from the Baltic sea. Biogeosciences. 2023;20(2):295–323.
52. Jørgensen BB, Weber A, Zopfi J. Sulfate reduction and anaerobic methane oxidation in black sea sediments. Deep Sea Res Part I. 2001;48(9):2097–120.
53. Fajković H. Influence of landfill site Baštijunski brig on the chemical composition of uppermost sediments of Vrana Lake in Ravni kotari area. PhD thesis, Faculty of Science, Zagreb; 2014.
54. Skennerton CT, et al. Methane-Fueled syntrophy through extracellular Electron transfer: Uncovering the genomic traits conserved within diverse bacterial partners of anaerobic methanotrophic Archaea. mBio. 2018;9(4):e00530–17.
55. Luek JL, Thompson KE, Larsen RK, Heyes A, Gonsior M. Sulfate reduction in sediments produces high levels of chromophoric dissolved organic matter. Sci Rep. 2017;7:8829.
56. Jilbert T, Cowie G, Lintumaki L. Anthropogenic inputs of terrestrial organic matter influence carbon loading and methanogenesis in coastal Baltic sea sediments. Front Earth Sci 2021; 9.
57. Liikanen A, Flöjt L, Martikainen P. Gas dynamics in eutrophic lake sediments affected by oxygen, nitrate, and sulfate. J Environ Qual. 2002;31:338–49.
58. van Grinsven S, et al. Redox zone and trophic state as drivers of Methane-Oxidizing bacterial abundance and community structure in lake sediments. Front Environ Sci. 2022;10:2296–X665.
59. Dar SA, Kleerebezem R, Stams AJM, Kuenen JG, Muyzer G. Competition and coexistence of sulfate-reducing bacteria, acetogens and methanogens in a lab-scale anaerobic bioreactor as affected by changing substrate to sulfate ratio. Appl Microbiol Biotechnol. 2008;78:1045–55.
60. Schorn S, et al. Persistent activity of aerobic methane-oxidizing bacteria in anoxic lake waters due to metabolic versatility. Nat Commun. 2024;15:5293.
61. Kevorkian R, Callahan S, Winstead R, Lloyd KG. ANME-1 archaea May drive methane accumulation and removal in estuarine sediments. Environ Microbiol Rep. 2021;13(2):185–94.
62. Wormald RM, Rout SP, Mayes W, Gomes H, Humphreys. PN. Hydrogenotrophic methanogenesis under alkaline conditions. Front Microbiol. 2020;11:1664–X302.
63. Zhang CJ, et al. Genomic and transcriptomic insights into methanogenesis potential of novel methanogens from Mangrove sediments. Microbiome. 2020;8:94.
64. Coskun ÖK, et al. Quantifying population-specific growth in benthic bacterial communities under low oxygen using H218O. ISME J. 2019;13:1546–59.
65. Zhang Z, et al. Evaluation of microbial assemblages in various saline-alkaline soils driven by soluble salt ion components. J Agric Food Chem. 2021;69:3390–400.
66. Yan W, et al. Metatranscriptomics-guided genome-scale metabolic reconstruction reveals the carbon flux and trophic interaction in methanogenic communities. Microbiome. 2024;12:121.
67. Meier D, et al. Hydrogen–independent CO2 reduction dominates methanogenesis in five temperate lakes that differ in trophic States. ISME Commun. 2024;4:1ycae089.
68. Nobu MK, et al. Catabolism and interactions of uncultured organisms shaped by eco-thermodynamics in methanogenic bioprocesses. Microbiome. 2020;8:111.
69. Ma KJ et al. Genomic and phylotypic properties of three novel marine bacteroidota from bare tidal flats reveal insights into their potential of polysaccharide metabolism. Front Mar Sci. 2023; 10.
70. Khomyakova MA, Merkel AY, Slobodkin AI. Anaerobaca lacustris gen. Nov., sp. Nov., an obligately anaerobic planctomycete of the widespread SG8-4 group, isolated from a coastal lake, and proposal of anaerobacaceae fam. Nov. Syst App Microbiol. 2024;47:4126522.
71. Payne PE et al. Uncovering novel functions of the enigmatic, abundant and active Anaerolineae in a salt marsh ecosystem. BioRxiv. 2024; 08.27.609934.
72. Liang QY et al. Niche modification by Sulfate-Reducing Bacteria drives microbial community assembly in anoxic marine sediments. mBio. 2023; 14(2).
73. Kleikamp HBC, et al. Comparative metaproteomics demonstrates different views on the complex granular sludge Microbiome. Wat Res. 2023;246:120700.
74. Wegener G, Krukenberg V, Riedel D, Tegetmeyer HE, Boetius A. Intercellular wiring enables electron transfer between methanotrophic archaea and bacteria. Nature. 2015;526(7574):587–90.
75. Slobodkin AI, et al. Composition and metabolic potential of Fe(III)-Reducing enrichment cultures of methanotrophic ANME-2a Archaea and associated Bacteria. Microorganisms. 2023;11(3):555.
76. Bouvier TC, Del Giorgio PA. Compositional changes in free-living bacterial communities along a salinity gradient in two temperate estuaries. Limnol Oceanogr. 2002;47(2):453–70.
77. Bremer E, Kramer R. Responses of microorganisms to osmotic stress. Annu Rev Microbiol. 2022;73:313–34.
78. Edmonds JW, Weston NB, Joye SB, Mou X, Moran MA. Microbial community response to seawater amendment in low-salinity tidal sediments. Microb Ecol. 2009;58(3):558–68.
79. Dong Y, et al. Eco-evolutionary strategies for relieving carbon limitation under salt stress differ across microbial clades. Nat Commun. 2024;15:6013.
80. Koenigshofer H, Loeppert HG. The up-regulation of proline synthesis in the meristematic tissues of wheat seedlings upon short-term exposure to osmotic stress. J Plant Physiol. 2019;237:21–9.
81. Ye P, et al. Proline utilization A controls bacterial pathogenicity by sensing its substrate and cofactors. Commun Biol. 2022;5:496.
82. Becker EA, et al. Phylogenetically driven sequencing of extremely halophilic archaea reveals strategies for static and dynamic osmo-response. PLOS Genet. 2014;10(11):e1004784.
83. Gregory GJ, Boyd EF. Stressed out: bacterial response to high salinity using compatible solute biosynthesis and uptake systems, lessons from Vibrionaceae. CSBJ. 2021;19:1014–27.

84. Gunde-Cimerman N, Plemenitaš A, Oren A. Strategies of adaptation of microorganisms of the three domains of life to high salt concentrations. FEMS Microbiol Rev. 2018;42(3):353–75.
85. Schwab L, et al. Sulfate reduction and homoacetogenesis at various hypersaline conditions: implications for H2 underground gas storage. Front Energy Res. 2023;11:2296–X598.

Publisher's note